ACS Catalysis

Research Article

pubs.acs.org/acscatalysis

# Exploring Small Bite-Angle Ligands for the Rhodium-Catalyzed Intermolecular Hydroacylation of β-S-Substituted Aldehydes with 1-Octene and 1-Octyne

Indrek Pernik, Joel F. Hooper, Adrian B. Chaplin,† Andrew S. Weller,* and Michael C. Willis

Department of Chemistry, University of Oxford, Chemistry Research Laboratory, Mansfield Road, Oxford, OX1 3TA, U.K.

Supporting Information

**ABSTRACT:** A comparative study of seven crystallographically characterized rhodium precatalysts, which contain a variety of chelating diphosphine ligands, for the hydroacylation of 1-octyne or 1-octene with 2-(methylthio)benzaldehyde has been undertaken. These studies show that the best performing catalyst for 1-octyne, $[Rh(L)(\eta^6\text{-}C_6H_5F)][BAr^F{}_4]$, L = $^iPr_2PNMeP^iPr_2$, delivers alkyne selective hydroacylation with high efficiencies at low loadings (1 mol %, 2.0 M aldehyde, 25 °C, ToN = 100, 97% conversion in 5 min), and also shows high selectivity for the linear product. Experiments suggest that the alkyne selectivity arises from the alkyne being more competitive for metal binding compared to the alkene. Labeling experiments using the $[Rh(^tBu_2PCH_2P^tBu_2)(\eta^6\text{-}C_6H_5F)][BAr^F{}_4]$ system, that gives the final product in a linear:branched ratio of 6:1, indicate that the pathway that produces the branched product operates via an irreversible hydride insertion. Intermediate acyl hydride complexes, $[Rh(L)(H)(COC_6H_4SMe)(acetone)][BAr^F{}_4]$, have been characterized by low temperature NMR spectroscopy, as have their subsequent reductive decarbonylation products, one of which has also been crystallographically characterized: $[Rh(^iPr_2PNMeP^iPr_2)(SMePh)(CO)][BAr^F{}_4]$.

[cat.] = Rh complex, 1 mol% selective for 1–octyne over 1–octene

**KEYWORDS:** *hydroacylation, rhodium, alkyne, alkene, diphosphine*

## INTRODUCTION

The atom-efficient coupling of an aldehyde and alkyne or an alkene to form a ketone, the hydroacylation reaction, is a potentially powerful transformation for organic and materials synthesis (Scheme 1).[1−5] These processes are often catalyzed by cationic rhodium bidentate phosphine fragments, $\{Rh(L)\}^+$ (L = bidentate phosphine), although neutral mono-dentate phosphine systems are also known.[6,7] The accepted mechanism, using $\{Rh(L)\}^+$ catalysts, is as outlined in Scheme 2, namely, C−H oxidative addition (**I**), alkene/alkyne coordination (**II**), hydride insertion (hydrometalation) to give linear (**III**) or branched (**IV**) intermediates, and turn-over limiting[2,8−10] reductive elimination. Alternative catalyst systems that operate via a similar mechanism have also been developed, for example those based upon $\{Rh(C_5Me_5)(PR_3)\}^+$.[11] Diene and alkyne hydroacylation mediated by neutral Ru-based catalysts have been reported, that operate via a distinctly different Ru-hydride mechanism.[1,12,13] Examples of carbonyl hydroacylation have also been reported.[14−16] Central to the development of many of these systems is balancing the requirements for active catalysts over the deleterious, irreversible, side reaction of reductive decarbonylation (**V**).

**Scheme 1. Hydroacylation**

We have recently reported on the ability to control the regioselectivity in this reaction with alkynes and β-substituted aldehydes, by judicious choice of the chelating phosphine in $\{Rh(L)\}^+$ catalysts,[17,18] and have also commented, along with others, on the underlying factors that might control this, being linked to the relative barriers of the hydride insertion step relative to the rate of reductive elimination of the respective intermediates.[6−8,11,17] A significant recent breakthrough in catalyst activity has been the use of small-bite angle chelating ligands, as developed by Hofmann[19−23] $R_2PCH_2PR_2$ (R = $^t$Bu, **A**; Cy, **B**; Scheme 3), that result in catalyst systems that can work at 0.1 mol % (cf. 5−10 mol % loadings that are generally used[1,2]) for a wide range of alkenes/alkynes and β-S-substituted aldehydes.[24] Although the reasons as to why these ligand systems support such efficient hydroacylation remain to be fully resolved, we speculate that reductive elimination is promoted by a combination of electronic and steric effects imposed by the small bite-angle ligand. Interestingly, we found that ligand **A** (R = $^t$Bu) was best in terms of the isolated yield of alkene hydroacylation product, while **B** (R = Cy) gave marginally

Received: August 9, 2012
Revised: November 5, 2012
Published: November 9, 2012

   dx.doi.org/10.1021/cs300541m | ACS Catal. 2012, 2, 2779−2786

**Scheme 2. General Mechanism for Hydroacylation**

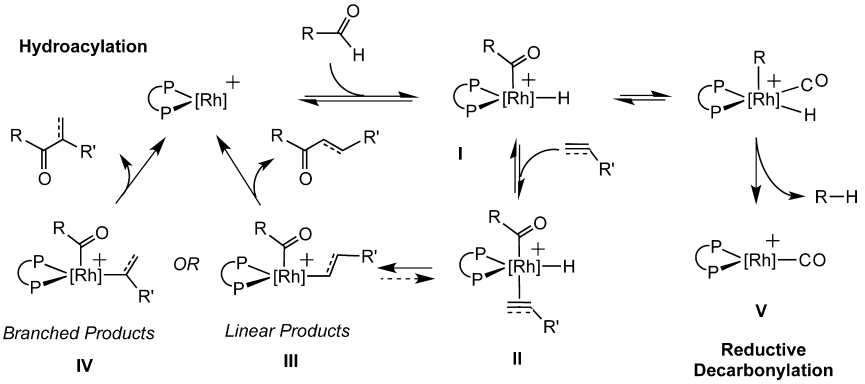


**Scheme 3. Ligands Used in This Study**

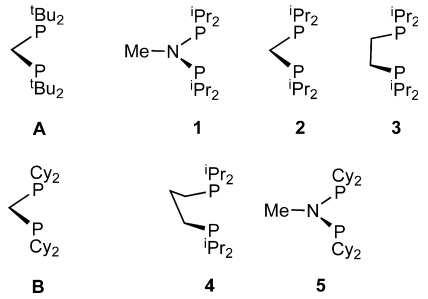


improved product yields for alkyne hydroacylation. That a mixed ligand system (R = $^t$Bu and Cy) afforded an intermediate result suggested that this was due to steric effects rather than the ligand intrinsic bite-angle. To probe this further we now report the use of $^i$Pr-substituted small-bite angle ligands with a variety of linking backbones ($C_1$, **2**; $C_2$, **3**; and $C_3$, **4**; Scheme 3) in the hydroacylation of the relatively demanding substrates 1-octene and 1-octyne with the $\beta$-S-substituted aldehyde 2-(methylthio)benzaldehdye. We also report use of the ligand $^i$Pr$_2$(NMe)P$^i$Pr$_2$, **1**, and its analogue Cy$_2$P(NMe)PCy$_2$ **5**, which are particularly interesting as small bite angle "PNP" ligands of this type have been used successfully in olefin oligomerization catalysis. The mechanism for this transformation is complex,[25−27] and the specific role of the ligand is yet to be fully delineated, although delocalization of the nitrogen lone pair in PNP-type ligands has been suggested to be important in the success of these ligands.[28] We show in this work that ligand **1** combined with a Rh-center supports fast alkyne (1-octyne) catalysis, with excellent linear to branched selectivity at relatively low catalyst loadings (1 mol %), and is also selective for alkyne over alkene hydroacylation. The mechanism of this process is also probed using deuterium-labeling experiments.

## RESULTS AND DISCUSSION

**Synthesis of Precatalysts and Stoichiometric Studies in Solution.** The ligands **1** to **3** were prepared by slight modifications of previously published routes.[29−31] Ligand **4** is commercially available, while **5** is a new ligand prepared analogously to **1** (see Supporting Information). Despite repeated attempts we have not been able to prepare $^t$Bu$_2$PNMeP$^t$Bu$_2$, which would provide a direct comparison with ligand **A**. These ligands can be isolated in moderate yield (50−70%) and high purity (by NMR spectroscopy). The corresponding rhodium precatalysts, [Rh(L)($\eta^6$-C$_6$H$_5$F)][BAr$^F_4$] **6a−10a**, (Ar$^F$ = 3,5-(CF$_3$)$_2$C$_6$H$_3$, L = **1−5**, Scheme 4) were prepared by addition of the appropriate ligand to [Rh(COD)$_2$][BAr$^F_4$] in C$_6$H$_5$F solvent and exposure to H$_2$ (4 atm). The new complexes (Scheme 4) were prepared in good yield (70−80%) as analytically pure microcrystalline solids. The time taken for the hydrogenation reaction is critical, leaving for longer than 2 h resulted in the formation of colloidal rhodium as evidenced by a black precipitate. In the solid-state these materials are bench-stable (there is no change by NMR spectroscopy after exposure of the solid to air for 24 h),

**Scheme 4. Fluorobenzene Adducts Prepared for This Study**[a]

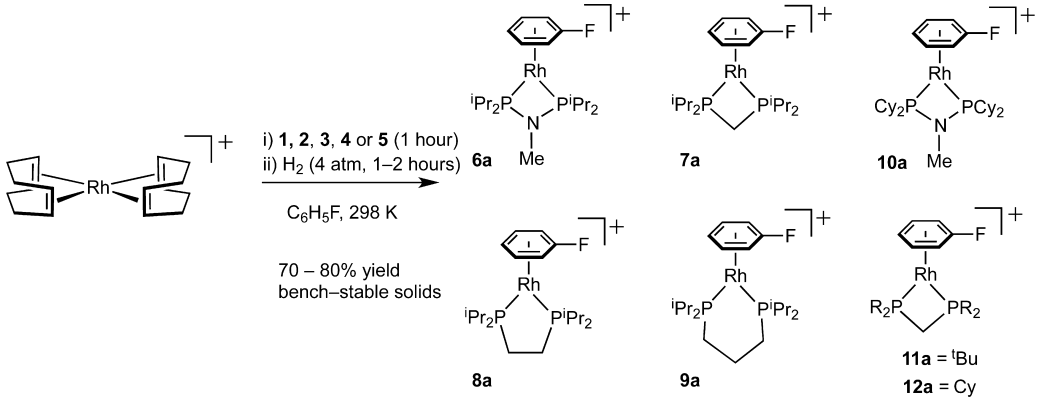


[a] [BAr$^F_4$]$^-$ anions are not shown.


dx.doi.org/10.1021/cs300541m | ACS Catal. 2012, 2, 2779−2786

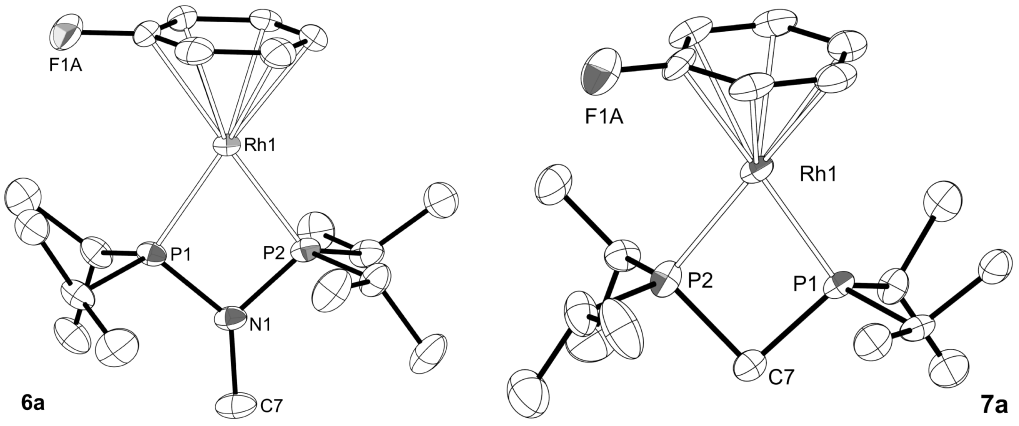


**Figure 1.** Solid-state molecular structures of complexes **6a** and **7a**. Displacement ellipsoids are shown at the 30% probability level. $[BAr^F_4]^-$ anions are not shown. Hydrogen atoms are not displayed. Only the major disordered components are shown.

**Table 1. Comparison of Selected Structural Metrics for Complexes 6a−10a**[a]

| | 6a | 7a | 8a | 9a | 10a |
|---|---|---|---|---|---|
| Rh1−P1/ Å | 2.2365(8) | 2.2244(11) | 2.2352(8) | 2.2556(8) | 2.2250(11) |
| Rh1−P2/ Å | 2.2103(8) | 2.2362(15) | 2.2399(8) | 2.2481(8) | 2.2267(11) |
| P1−Rh1−P2/ deg | 70.36(3) | 72.64(5) | 84.81(3) | 93.78(3) | 70.49(4) |
| P1−C/N−P2/ deg | 98.33(13) | 91.8(2) | n/a | n/a | 98.33(17) |
| av. Rh−C(arene)/ Å | 2.313 | 2.337 | 2.325 | 2.331 | 2.315 |
| Rh−(arene) range/ Å | 2.297(5)−2.329(5) | 2.313(8)−2.362(8) | 2.297(4)−2.353(6) | 2.285(3)−2.395(3) | 2.282(4)−2.339(5) |

[a]See Scheme 4 for numbering.

**Scheme 5. $[BAr^F_4]^-$ Anions Not Shown**

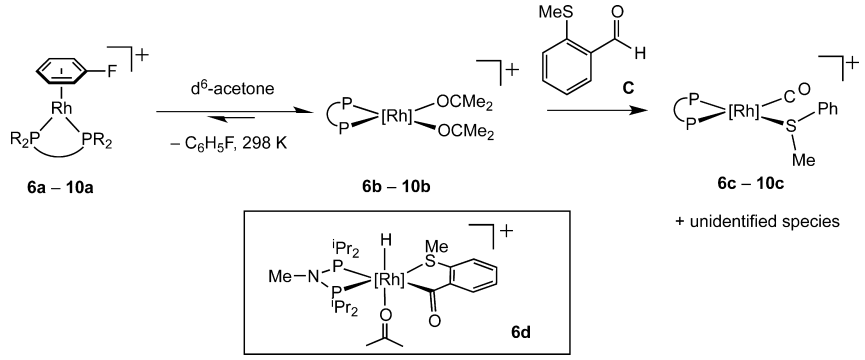


although they are best stored under an inert atmosphere. In our hands, use of the corresponding norbornadiene precursors led to impure materials. This preparative route, and stability of the fluorobenzene adducts, mirrors that reported for the analogous complexes formed with ligands **A** and **B**: **11a** and **12a** (Scheme 4) respectively.[24]

The solution NMR data for the new complexes **6a−10a** all show single environments in their $^{31}P\{^1H\}$ NMR spectra that also display coupling to $^{103}Rh$ [$J$(RhP) 175−205 Hz]. In their $^1H$ NMR spectra ($C_6H_5F$ solution) signals due to the phosphine, $[BAr^F_4]^-$ anion and coordinated $C_6H_5F$, the latter shifted up-field from free ligand [e.g., **6a** $\delta$ 6.22 (2H), 6.10 (2 H), 5.49 (1 H)], are observed. Electrospray ionization mass spectrometry (ESI-MS[32]) confirms the coordination of fluorobenzene in the parent ions. The solid-state structures of **6a−10a** have been determined, are unremarkable, and are fully consistent with the solution NMR data and are very similar to those reported for ligands **A** and **B**[24] (Figure 1 for complexes **6a** and **7a**, Table 1, Supporting Information for **8a**, **9a** and **10a**). A small number of solid-state structures of PNP ligands with Rh have been reported previously.[33−35]

As hydroacylation catalysis is often performed in acetone solution, as it can provide stabilization toward reductive decarbonylation by occupying a vacant site on the metal center,[24] we have explored the coordination chemistry of **6a−10a** in this solvent. When dissolved in $d_6$-acetone free fluorobenzene is observed [7.40 (2H), 7.21 1 (1 H), 7.12 (2 H)], and there is only a small chemical shift change of the single environment observed in the $^{31}P\{^1H\}$ NMR spectra. These data assign these complexes to the acetone adducts $[Rh(L)(acetone)_2][BAr^F_4]$ **6b−10b** (Scheme 5). Complexes **6b**, **7b**, and **10b** are observed to be in equilibrium with the fluorobenzene adducts (**6a**, **7b**, and **10a**), with the acetone adducts significantly favored. Interestingly, for the wider bite-angle ligands (complexes **8a** and **9a**) only the acetone adducts are observed, suggesting relatively weaker binding of fluorobenzene. Similar acetone adducts have been prepared for **11a** and are also in equilibrium with the fluorobenzene


dx.doi.org/10.1021/cs300541m | ACS Catal. 2012, 2, 2779−2786

complexes.[24] Addition of the β-S-substituted aldehyde 2-(methylthio)benzaldehdye, **C**, to acetone solutions of **6b**−**10b** ultimately resulted in the formation of the reductive decarbonylation products [Rh(L)(SMePh)(CO)][$BAr^F_4$] **6c**−**10c**. These products were identified by $^{31}P\{^1H\}$ NMR spectroscopy and ESI-MS. In particular a set of doublet of doublets [e.g., **6c**, δ 91.4 *J*(RhP) 125, *J*(PP) 59 Hz; δ 69.5 *J*(RhP) 114, *J*(PP) 59 Hz] are observed in the $^{31}P\{^1H\}$ NMR spectrum and no corresponding hydrides were observed in the $^1H$ NMR spectrum. These data are consistent with other Rh(I) reductive decarbonylation products of aldehyde **C**.[24,36] The solid-state structure of **6c** has been determined and shows a pseudo square planar Rh(I) center, as expected (Figure 2).[24,36] These decarbonylation products are inactive as catalysts in the hydroacylation reaction (vide infra).

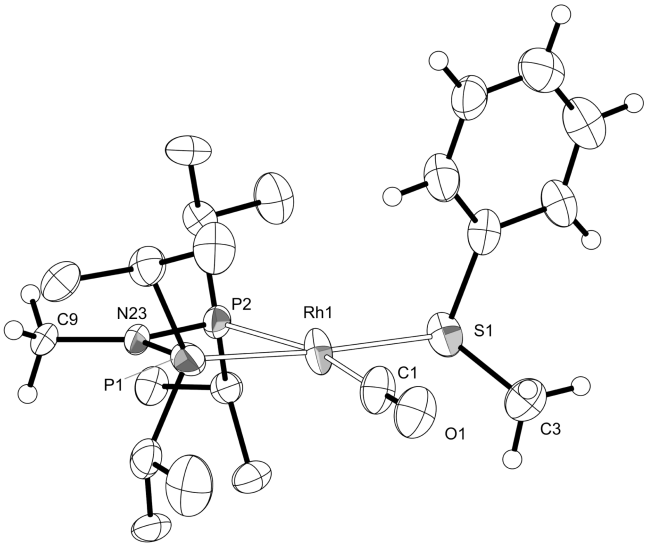


**Figure 2.** Solid-state molecular structure of complex **6c**. Displacement ellipsoids are shown at the 30% probability level. [$BAr^F_4$]$^-$ anion and most hydrogen atoms are not shown. Major disordered components shown only. Selected bond lengths (Å) and angles (deg): Rh1−C1, 1.889(10); Rh1−S1, 2.3753(16); Rh1−P1, 2.2394(14); Rh1−P2, 2.3310(15); P1−Rh1−S1, 170.38(7); P2−Rh1−C1, 165.7(3); P1−N23−P2, 102.7(2); P1−Rh1−P2, 70.24(6).

The formation of the reductive decarbonylation products presumably occurs via initial oxidative addition of aldehyde **C** to the acetone adducts to form a transient acyl-hydride. Following the reaction of **6b** with **C** by $^1H$ NMR spectroscopy at 25 °C ($d_6$-acetone) indicates the immediate (on time of mixing) formation of an acyl-hydrido species tentatively identified as [Rh($^i$Pr$_2$P(NMe)P$^i$Pr$_2$)(H)(COC$_6$H$_4$SMe)-(acetone)][$BAr^F$], **6d**, (inset Scheme 5) by the observation of a broad hydride signal at δ −20.22 similar to that observed for the analogous complex with ligand **A** (δ −20.29). The $^{31}P\{^1H\}$ NMR spectrum was broad and uninformative at this temperature. Rapid cooling (−60 °C) of a freshly prepared solution reveals a $^1H$ NMR spectrum that shows a hydride environment at δ −20.09 as a doublet of doublet of doublets, showing coupling to two *cis* $^{31}P$ environments and one $^{103}Rh$, as confirmed by $^{31}P$ decoupling experiments. The $^{31}P\{^1H\}$ NMR spectrum at this temperature shows two environments, one of which shows a particularly small $^{31}P$-$^{103}Rh$ coupling constant, consistent with a Rh(III) center and one phosphine being *trans* to a high-*trans* influence acyl ligand: δ 92.2 [*J*(RhP) 133 Hz], 83.5 [*J*(RhP) 63 Hz]. Again, these data are very similar to that reported for the analogous acyl hydride system using ligand **A**.[24] **6d** decays rapidly at 25 °C (50% consumption after 5 min) to give **6c**, a time scale significantly faster than the system with ligand **A**,[24] that has $t_{1/2}$ = 1.79 h for a first order process. Other hydrido species are formed in parallel alongside the reductive decarbonylation products, and we speculate that these might be due to C−H activation of the $^i$Pr group.[37,38] For this reason simple first order kinetics were not observed for decarbonylation to give **6d**. Similar behavior and rapid decarbonylation was also observed for **7b** when combined with **C**. Although not straightforward, what is clear is that when comparing similar ligands (e.g., **A** with **1** or **2**) then decomposition (reductive decarbonylation) is faster for the $^i$Pr-based ligands (**1** and **2**) compared to the $^t$Bu-substituted ligands (**A**). As to why decarbonylation is faster, steric effects could well play a part; while the observation of hydride co-products with these $^i$Pr-based ligands might point to intermediates with agostic C−H interactions that have been suggested to lower the barrier to reductive elimination processes.[39] The rapid decarbonylation of these small bite angle ligand complexes can also be contrasted to the {Rh(DPEphos)}$^+$ system in which the hemilabile ligand attenuates decarbonylation by occupying a vacant site on the metal center ($t_{1/2}$ = 160 h).[36]

**Catalysis.** To determine the effect of phosphorus substituent and backbone linker (NMe versus $CH_2$) the precatalysts **6a**, **7a**, and **10a** were screened in the hydroacylation reaction of 1-octene or 1-octyne with aldehyde **C** (Table 2). Also compared are the previously reported catalysts **11a** and **12a**.[24] Catalysts were initially compared under the conditions of 10 mol % loading, 0.075 M aldehyde, using dichloroethane (DCE) as a solvent. As 1-octene hydroacylation proceeds slowly at 25 °C, higher temperatures were used (80 °C, as previously reported[24]). For all but **11a** the alkyne reacts considerably faster than the alkene. In contrast under these conditions **11a** is considerably more efficient for alkene hydroacylation, and poorer for alkynes, as previously noted.[24] Use of acetone as a solvent affords no significant difference to DCE (Entries 11 and 12) under these conditions of relatively high catalyst loading. These preliminary results demonstrate that the -$^i$Pr (and -Cy) substituted systems are not only good hydroacylation catalysts, but favor alkyne hydroacylation over alkene. We briefly screened the use of untethered aldehydes (i.e., benzaldehyde), but this resulted in no productive reaction presumably because of rapid decarbonylation.

With the preference for alkyne over alkene hydroacylation established using the $^i$Pr ligands, we focused on optimizing the reactivity of **C** with 1-octyne as an exemplar, as 1-octene hydroacylation using **11a** and **C** is already established.[24] Table 3 presents comparative studies using the optimized conditions developed previously[24] (1 mol % loadings, 2.0 M aldehyde, 25 °C, aldehyde:alkyne 1:1.5). These data show that when comparing ligands with both $^i$Pr and Cy groups, improved conversions of substrate to product are obtained with NMe backbones compared with $CH_2$ (entries 1−4). However only with ligand **1** (i.e., **6a**) is 100% conversion achieved (entry 1). Figure 3 shows the concentration/time plots for these reactions, which demonstrate that although all the catalysts initially turnover rapidly, deactivation (presumably by reductive decarbonylation and otherwise) results in catalyst death for **7a**, **10a**, and **12a**. Under these conditions, catalysis using **6a** is essentially complete by the first measured time point (ToN = 97, 5 min), which, along with **8a** (vide infra) is the fastest we


dx.doi.org/10.1021/cs300541m | *ACS Catal.* 2012, 2, 2779−2786

**Table 2. Comparison of PNP($^i$Pr), PCP($^i$Pr), PCP(Cy), and PCP($^t$Bu) Systems in the Hydroacylation of 1-Octene or 1-Octyne with C[a]**

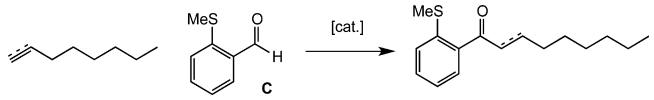


| entry | catalyst | substrate | conversion/%[b] | time (min) | solvent | temperature/ °C |
|---|---|---|---|---|---|---|
| 1 | PNP($^i$Pr) **6a** | 1-octene | 66 | 60 | DCE | 80 |
| 2 | PNP($^i$Pr) **6a** | 1-octyne | 100 | 5 | DCE | 25 |
| 3 | PCP($^i$Pr) **7a** | 1-octene | 67 | 60 | DCE | 80 |
| 4 | PCP($^i$Pr) **7a** | 1-octyne | 100 | 5 | DCE | 25 |
| 5 | PNP(Cy) **10a** | 1-octene | 40 | 120 | DCE | 80 |
| 6 | PNP(Cy) **10a** | 1-octyne | 97 | 5 | DCE | 25 |
| 7 | PCP($^t$Bu) **11a** | 1-octene | 94 | 15 | DCE | 80 |
| 8 | PCP($^t$Bu) **11a** | 1-octyne | 90 | 360 | DCE | 25 |
| 9 | PCP(Cy) **12a** | 1-octene | 91 | 60 | DCE | 80 |
| 10 | PCP(Cy) **12a** | 1-octyne | 95 | 15 | DCE | 25 |
| 11 | PNP($^i$Pr) **6a** | 1-octene | 64 | 60 | acetone | 55 |
| 12 | PNP($^i$Pr) **6a** | 1-octyne | 100 | 5 | acetone | 25 |

[a]Conditions: 0.075 M aldehyde, 10 mol % catalyst. Aldehdye: akyne/alkene ratio =1:1.5. [b]Conversions measured by HPLC.

**Table 3. Comparison of R-Group on Ligands and Chelate Linker Length[a]**

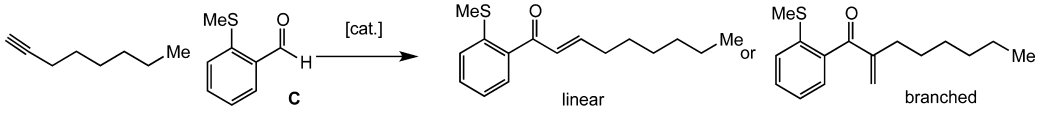


| entry | catalyst | P−Rh−P bite angle/deg | conversion/% (5 min) | conversion/% (120 min) | linear:branch ratio |
|---|---|---|---|---|---|
| 1 | PNP($^i$Pr) **6a** | 70.3 | 97 | 100 (98)[c] | 21:1 |
| 2 | PCP($^i$Pr) **7a** | 72.6 | 77 | 81 | 12:1 |
| 3 | PNP(Cy) **10a** | 70.4 | 68 | 77 | 69:1 |
| 4 | PCP(Cy) **12a** | 72.8[b] | 55 | 60 | 10:1 |
| 5 | PCP($^t$Bu) **11a** | 74.6[b] | 74 | 99 | 6:1 |
| 6 | PCCP($^i$Pr) **8a** | 84.8 | 100 | 100 (98)[c] | 16:1 |
| 7 | PCCCP($^i$Pr) **9a** | 93.7 | 63 | 100 (96)[c] | 11:1 |

[a]1-octyne with **C**, 25 °C 2.0 M aldehyde, 1 mol % catalyst, acetone solvent. Aldehdye:alkyne ratio = 1:1.5. Conversions and linear:branched ratios were measured by HPLC. [b]See reference 24. [c]Isolated yields are given in parentheses.

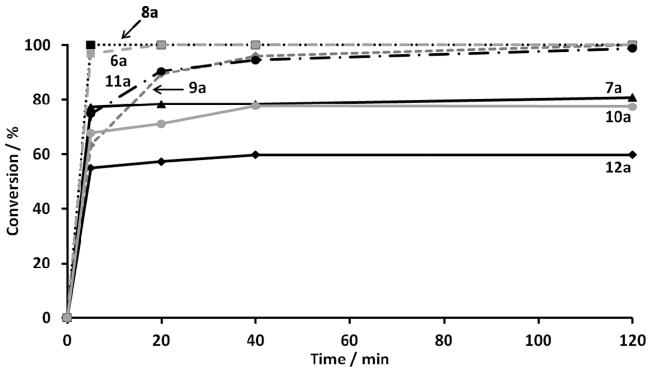


**Figure 3.** Hydroacylation product formation with respect to time for **6a** (gray squares), **7a** (black triangles), **8a** (black squares), **9a** (gray diamonds), **10a** (gray circles), **11a** (black circles), **12a** (black diamonds) for the reaction of **1**-octyne with aldehyde **C**. 1.0 mol % catalyst loading, acetone, 25 °C, 2.0 M aldehyde, acetone solvent, Aldehdye:alkyne ratio = 1:1.5. Conversions were measured by HPLC.

have yet measured for the hydroacylation of either alkenes or alkynes using aldehydes such as **C**.[24] Linear: branched selectivity is best for **10a** (69:1), good for **6a** (21:1) and poorest for **11a** (6:1). The wider bite angle ligands **8a** and **9a** also show reasonable selectivity for linear product and both return 100% conversion, this latter point indicating a relative resistance to decarbonylation. Interestingly **8a**, which has a smaller bite angle to **9a**, is much faster, being comparable to **6a**. Under these conditions, **11a** ($^t$Bu) also effects complete conversion but more slowly than for **6a** (ToN = 100, 120 min). That this catalyst is also long-lived (Figure 3) reflects the relative resistance to decarbonylation for the $^t$Bu ligand compared with $^i$Pr, cf **7a**, as previously noted. Apart from the positive effect of the NMe backbone there is no clear trend apparent from variation of these ligands. As relative rates and selectivities will be determined by the hydride insertion step coupled with relative rates of reductive elimination of final product, both of which will be affected by the electronic and steric demands of the ligand,[40,41] the situation is clearly finely balanced and nuanced. Nevertheless, what is clear is that for these ligands studied, **6a** gives the best conversion, overall rate, and selectivity for alkyne hydroacylation.

Although turnover is fast at 2.0 M aldehyde concentration and 25 °C, catalyst **6a** will also operate effectively at 1 mol % at lower concentration regimes and temperatures (0 °C): 0.1 M (ToN = 95, 3.5 h) and 0.4 M (ToN = 94, 1.7 h). We have previously shown that the combination of acetone solvent and MeCN coligand (2 equiv) acts to stabilize decarbonylation and increase the rate of catalysis allowing for low catalyst loadings of 0.1 mol % in 1-octene hydroacylation using **C** and **11a**.[24] For


dx.doi.org/10.1021/cs300541m | ACS Catal. 2012, 2, 2779−2786

**Scheme 6. D-Labeling Experiments**

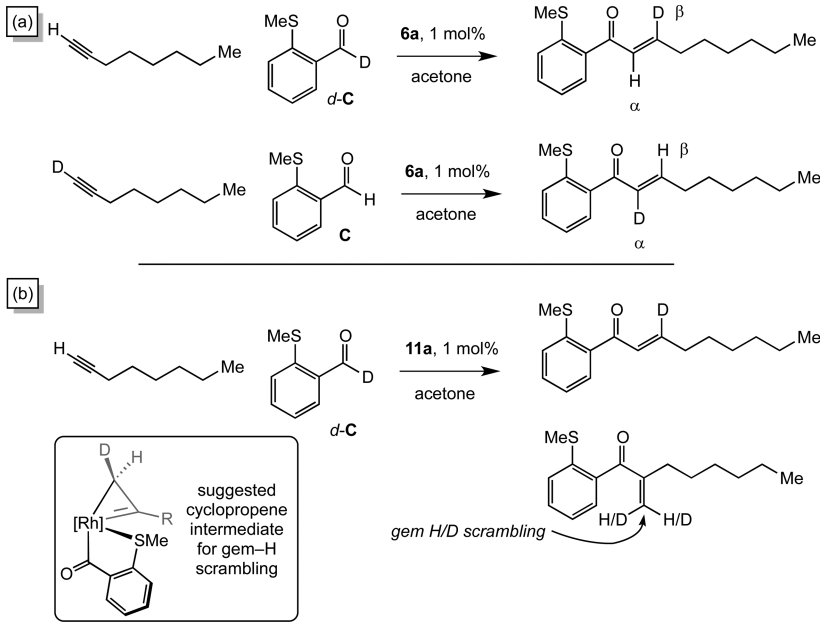


**6a** loadings cannot be pushed below 0.5 mol % (2.0 M aldehyde, 25 °C, 2 equiv of MeCN) without a drop in conversion (e.g., 0.4 mol %, 87% conversion; 0.1 mol %, 50% conversion). The higher loadings required using **6a** compared to **11a** perhaps reflect the faster reductive decarbonylation of the former catalyst. Because of this rapid decarbonylation a satisfactory fit for the growth of product for a number of simple kinetic scenarios was not obtained, as the catalyst concentration is decreasing significantly with time. Using *d*-1-octyne (1.0 mol %, 0.1 M, 0 °C) resulted in effectively no change in overall time for full conversion (ToN = 100, 3.3 h). Use of *d*-**C** gave a slower turnover (ToN = 68, 5 h). By using the initial rate method for **C** and *d*-**C** substrates, a KIE of 1.6 ± 0.2 was measured. We have previously found that **11a** operates under pseudo first order conditions for alkene hydroacylation using **C** and shows a similar, small, KIE (1.4 ± 0.2)[24] while for the {Rh(DPEphos)}$^+$ system alkyne hydroacylation with **C** shows a negligible KIE (1.1 ± 0.1), and reductive elimination is turnover limiting.[8] In the system here the modest KIE suggests that irreversible aldehyde oxidative addition is not rate-limiting (i.e., **I**, Scheme 2). However these data do not allow us to discriminate between hydride insertion or reductive elimination being turnover limiting. It is interesting to note that Dong and co-workers have recently suggested that hydride insertion in *linear* intermolecular alkene hydroacylation using salicylaldehyde is turnover limiting,[6] while Hofmann and co-workers have demonstrated increased barriers to alkyl migration in the small bite angle system Rh($^t$Bu$_2$PCH$_2$P$^t$Bu$_2$)(neopentyl)($\eta^2$-H$_2$C = CH$_2$).[19] A small KIE (1.22 ± 0.11) similar to that reported here has been also reported for the hydride migration step in the hydroformylation of 1-octene using Rh-Xantphos complexes.[42] Probing the reaction of 1-octyne and **C** with **6a** as a catalyst using initial rates (1.0 mol %; 0.001 M **6a**; aldehyde:alkene ratio 1:1.5; 0 °C; initial rate = 1.3 ± 0.4 × $10^{-3}$ M $s^{-1}$, ToN = 100) resulted in a positive order of reaction with respect alkyne (10-fold excess; initial rate = 4.0 ± 0.2 × $10^{-3}$ M $s^{-1}$, ToN = 96) while excess of **C** suppressed catalysis (10-fold excess; initial rate =0.4 ± 0.2 × $10^{-3}$ M $s^{-1}$, ToN = 79), to the extent that complete conversion was not achieved. Suppression of productive hydroacylation catalysis by excess aldehyde has recently been noted as being due to irreversible reductive decarbonylation of the catalyst, and we suggest a similar scenario could be operating here.[6] Given the rapid rate of catalyst decomposition for the systems described in this paper we are reluctant to interpret our data further.

These isotope experiments, however, do shed some light on aspects of the mechanistic pathway. Using 1-octyne, *d*-**C** and **6a** (which gives linear product in excellent selectivity, Table 3) deuteration was observed exclusively in the $\beta$-position of the final product (Scheme 6a), as expected for hydride insertion into the alkyne (e.g., **III**, Scheme 2). Likewise use of *d*-1-octyne afforded exclusive D-incorporation at the $\alpha$-position. Similar results have been reported for the alkyne hydroacylation and the {Rh(DPEphos)}$^+$ system,[8] whereas for linear-selective alkene hydroacylation using **11a** and *d*-**C** incorporation of deuterium into both $\alpha$- and $\beta$-positions occurred because of reversible insertion/$\beta$-elimination.[24] For alkyne insertion, in the absence of stable intermediates, it is difficult to probe such a reversible process for linear selectivity,[43] as the corresponding alkenyl intermediate (**III**, Scheme 2) would undergo $\beta$-hydrogen elimination to give the same product with no opportunity for deuterium-scrambling. We have shown, however, that for the {Rh(DPEphos)}$^+$ system kinetic modeling supports that the insertion for both linear and branched alkenyl intermediates is irreversible. These studies also showed that scrambling of the gem-positions in the branched alkenyl intermediate occurs (**IV** Scheme 2) and was suggested to occur via a metallocyclopropene intermediate (inset Scheme 6).[8] Using catalyst **11a** with *d*-**C** and 1-octyne, which shows a linear to branched ratio of 6:1, allows the reversibility of the branched process to be probed in these small bite-angle systems by utilizing this gem-H scrambling. This is because if the branched-alkenyl intermediate (**IV**, Scheme 2) undergoes an isomerization process that scrambles the gem-H/D, and if this is also followed by $\beta$-elimination and subsequent insertion to give the linear product, this would place deuterium in the $\alpha$-position of the resulting ketone. Experimentally this is not observed, with only deuteration in the $\beta$-position of the


dx.doi.org/10.1021/cs300541m | *ACS Catal.* 2012, 2, 2779–2786

linear product occurring. Importantly H/D scrambling of the gem-positions in the (minor) branched product is observed (Scheme 6b), showing that the isomerization process is operating even if $\beta$-elimination is not. These observations demonstrate that hydride insertion is not reversible for the branched pathway. Reversible hydride insertion with alkynes is rare.[44]

The catalyst resting state at low temperature was revealed by addition of **C**/1-octyne to **6a** (in $d^6$-acetone, 10 mol %) at −80 °C, this temperature used to slow the rapid turnover at this high loading which in turn is necessary for the observation of intermediates by NMR spectroscopy. $^{31}P\{^1H\}$ and $^1H$ NMR data suggest the formation of the linear product-bound to the metal center, $[Rh(^iPr_2P(NMe)P^iPr_2)(\kappa^2\text{-}O,S\text{-}CO(C_6H_4SMe)\text{-}(CH{=}CH(CH)_5Me)][BAr^F]$ **13** by a pair of doublet of doublets showing coupling to $^{103}Rh$ (indicative of coupling to a Rh(I) center) and mutual $^{31}P$ coupling.[45] ESI-MS experiments during catalysis show the only organometallic species observed to have a mass and isotopic distribution fully consistent with **13** ($m/z$ = 628.21, calc. 628.24). Related complexes using the $\{Rh(o\text{-}^iPrC_6H_4)_2PCH_2CH_2(o\text{-}^iPrC_6H_4)_2\}$ fragment have been reported previously.[17] The acyl-hydride **6d** was not observed under these conditions of turnover, in either the $^{31}P\{^1H\}$ NMR spectrum or the high-field region of the $^1H$ NMR spectrum. Complex **13** can also be directly prepared on addition of the linear hydroacylation product to **6a** (*E*-1-(2-methylthio)-phenyl)non-2-ene-1-one). On warming to room temperature complete conversion of the aldehyde is observed (by $^1H$ NMR spectroscopy) to give the final product; while at this temperature broad signals between $\delta$ 85 and 70 are observed in the $^{31}P\{^1H\}$ NMR spectrum. Addition of excess **C** to this solution resulted in rapid reductive decarbonylation to give **6c**.

Selectivity for alkyne hydroacylation over alkene using **C** and **6a** as a catalyst is demonstrated by a direct competition experiment (1 mol %, 0.4 M aldehyde, 0 °C) in which a 1:1 mixture of 1-octyne and 1-octene were subjected to catalysis. This produced no alkene hydroacylation, while complete alkyne hydroacylation occurred in 30 min (ToN = 50). Under the same conditions (1 mol % **6a**, 0.4 M aldehyde, 0 °C) but now using a large excess of alkene and alkyne (**C**: 1-octyne: 1-octene = 1: 5: 5) also showed no alkene hydroacylation. Changing the temperature to 25 °C results in a small amount (less than 5% over 2 h) of alkene hydroacylation that only starts once about 90% alkyne is consumed (ca. 5 min). Clearly there is some catalyst decomposition over this period, as the control experiment of 100% 1-octene (1 mol %, 0.4 M aldehyde, 0 °C) showed increased consumption of alkene (ca. 20%) over a similar time period (2 h). These results suggest that the alkyne is competing effectively for the metal center coordination compared with the alkene. This impressive selectivity for alkyne over alkene hydroacylation mirrors that observed for the relative rates of hydrogenation of alkynes and alkenes mediated by the closely related Schrock/Osborne $[Rh(PR_3)_2(H)_2(solvent)_2]^+$ catalyst systems, in which selective alkyne hydrogenation is observed.[46] Further evidence for this selectivity arising from competitive metal binding is given by use of *d*-**C**, a 1:1 mixture of 1-octyne and 1-octene and **6a** (0 °C, 0.4 M, 1 mol % total loading). For this mixture exclusive deuteration in the $\beta$-position is observed in the alkyne hydroacylation product. If reversible alkene coordination/hydride insertion were occurring to any significant extent H/D exchange, as established for **11a**, *d*-**C** and 1-octene,[24] would result in incorporation of H into the acyl hydride (rather than starting deuteride) and thus observation of H in the $\beta$-position of the product (Scheme 7). The control experiment using **6a**, *d*-

**Scheme 7. Mechanistic Scenario for Reversible Alkene Insertion Followed by Productive Alkyne Hydroacylation**[a]

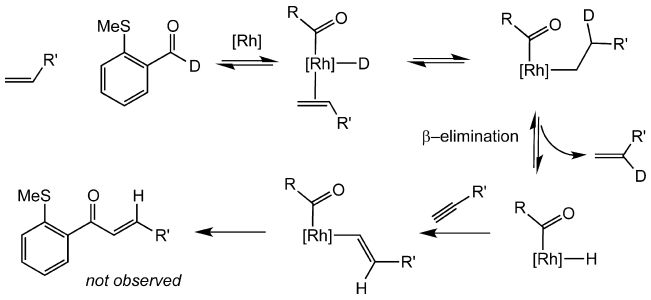


[a]R = $C_6H_4SMe$; R′ = hexyl.

**C** and 1-octene resulted of incorporation of deuterium into both $\alpha$- and $\beta$-positions of the final product of alkene hydroacylation, demonstrating H/D exchange and thus reversible alkene insertion in the absence of alkyne. Finally, the time to completion for the alkyne hydroacylation in this competition experiment using **C** is effectively half that observed for 100% alkyne at 1 mol % catalyst (cf. ToN 50, 30 min versus ToN = 94, 1.7 h), consistent with the effective doubling of catalyst loading and no inhibition from coordination of excess alkene.

## CONCLUSIONS

We have shown that a rhodium catalyst based upon the small bite-angle ligand $^iPr_2P(NMe)P^iPr_2$ will mediate the hydroacylation of 1-octyne with 2-(methylthio)benzaldehdye with high efficiencies, at low loadings (1 mol %), and with high selectivity for the linear product. This catalyst also shows excellent selectivity for alkynes (1-octyne) over alkenes (1-octene), and experiments suggest that the selectivity arises from the alkyne being competitive for metal binding over the alkene. Labeling experiments using the catalyst formed with $^tBu_2PCH_2P^tBu_2$ (**11a**) also indicate that the pathway that produces the branched product operates via an irreversible hydride insertion. Comparison with other small bite angle ligands with $CH_2$ or NMe linkers and $^i$Pr or Cy groups in the phosphine shows that the $^iPr_2P(NMe)P^iPr_2$ ligand is the best in terms of optimizing conversion, overall rate, and selectivity for 1-octyne hydroacylation. However, this fast rate comes at the cost of relatively rapid catalyst deactivation via decarbonylation compared to other systems, for example, $^tBu_2PCH_2P^tBu_2$, **A**. That longer backbone linkers in the phosphine ($CH_2CH_2$) and ($CH_2CH_2CH_2$) are also effective catalysts for 1-octyne hydroacylation makes simple correlations between electronic (bite angle) and steric (phosphine substituents) difficult with this present set of data. This aside, these new catalyst systems demonstrating very fast catalysis (1 mol %, ToN 100, 5 min) for alkyne hydroacylation add to the tool box of catalysts available for the intermolecular hydroacylation of $\beta$-substituted aldehydes: linear-[18] and branched-selective[17] coupling with alkynes and linear-selective alkene hydroacylation.[24] Fully teasing out the factors that control selectivity, in particular branched-selective alkene hydroacylation, and removing the $\beta$-substituted tether are our future goals.


dx.doi.org/10.1021/cs300541m | ACS Catal. 2012, 2, 2779–2786

## ■ ASSOCIATED CONTENT

### Supporting Information

Experimental procedures and compound characterization data, crystallographic data collection, and refinement details. This material is available free of charge via the Internet at http://pubs.acs.org. Crystallographic data have also been deposited with the Cambridge Crystallographic Data Center (CCDC: 894726−894731) and can be obtained via www.ccdc. cam.ac.uk/data_request/cif.

## ■ AUTHOR INFORMATION


### Corresponding Author

*E-mail: andrew.weller@chem.ox.ac.uk.

### Present Address

[†]Department of Chemistry, University of Warwick, Warwick, CV34 7AL, U.K.


### Notes

The authors declare no competing financial interest.

## ■ ACKNOWLEDGMENTS

The EPSRC for funding (J.F.H., A.B.C.), Archimedes Foundation (Estonia) for a Ph.D. Scholarship (I.P.).

## ■ REFERENCES


(1) Leung, J. C.; Krische, M. J. *Chem. Sci.* **2012**, *3*, 2202−2209.
(2) Willis, M. C. *Chem. Rev.* **2009**, *2010*, 725−748.
(3) Jun, C. H.; Jo, E. A.; Park, J. W. *Eur. J. Org. Chem.* **2007**, 1869−1881.
(4) Bosnich, B. *Acc. Chem. Res.* **1998**, *31*, 667−674.
(5) Biju, A. T.; Kuhl, N.; Glorius, F. *Acc. Chem. Res.* **2011**, *44*, 1182−1195.
(6) von Delius, M.; Le, C. M.; Dong, V. M. *J. Am. Chem. Soc.* **2012**, *134* (36), 15022−15032.
(7) Coulter, M. M.; Kou, K. G. M.; Galligan, B.; Dong, V. M. *J. Am. Chem. Soc.* **2010**, *132*, 16330−16333.
(8) Pawley, R. J.; Huertos, M. A.; Lloyd-Jones, G. C.; Weller, A. S.; Willis, M. C. *Organometallics* **2012**, *31*, 5650−5659.
(9) Fairlie, D. P.; Bosnich, B. *Organometallics* **1988**, *7*, 946−954.
(10) Dong and co-workers have recently reported that hydride insertion can be turnover limiting in certain cases, see reference 6.
(11) Roy, A. H.; Lenges, C. P.; Brookhart, M. *J. Am. Chem. Soc.* **2007**, *129*, 2082−2093.
(12) Shibahara, F.; Bower, J. F.; Krische, M. J. *J. Am. Chem. Soc.* **2008**, *130*, 14120−14122.
(13) Omura, S.; Fukuyama, T.; Horiguchi, J.; Murakami, Y.; Ryu, I. *J. Am. Chem. Soc.* **2008**, *130*, 14094−14095.
(14) Shen, Z.; Dornan, P. K.; Khan, H. A.; Woo, T. K.; Dong, V. M. *J. Am. Chem. Soc.* **2009**, *131*, 1077−1091.
(15) Khan, H. A.; Kou, K. G. M.; Dong, V. M. *Chem. Sci.* **2011**, *2*, 407−410.
(16) Pawley, R. J.; Moxham, G. L.; Dallanegra, R.; Chaplin, A. B.; Brayshaw, S. K.; Weller, A. S.; Willis, M. C. *Organometallics* **2010**, *29*, 1717−1728.
(17) González-Rodríguez, C.; Pawley, R. J.; Chaplin, A. B.; Thompson, A. L.; Weller, A. S.; Willis, M. C. *Angew. Chem., Int. Ed.* **2011**, *50*, 5134−5138.
(18) Poingdestre, S.-J.; Goodacre, J. D.; Weller, A. S.; Willis, M. C. *Chem. Commun.* **2012**, *48*, 6354−6356.
(19) Urtel, H.; Meier, C.; Rominger, F.; Hofmann, P. *Organometallics* **2010**, *29*, 5496−5503.
(20) Eisentrager, F.; Gothlich, A.; Gruber, I.; Heiss, H.; Kiener, C. A.; Kruger, C.; Ulrich Notheis, J.; Rominger, F.; Scherhag, G.; Schultz, M.; Straub, B. F.; Volland, M. A. O.; Hofmann, P. *New J. Chem.* **2003**, *27*, 540−550.
(21) Urtel, H.; Meier, C.; Eisentrager, F.; Rominger, F.; Joschek, J. P.; Hofmann, P. *Angew. Chem., Int. Ed.* **2001**, *40*, 781−784.
(22) Hofmann, P.; Meier, C.; Hiller, W.; Heckel, M.; Riede, J.; Schmidt, M. U. *J. Organomet. Chem.* **1995**, *490*, 51−70.
(23) Hofmann, P.; Meier, C.; Englert, U.; Schmidt, M. U. *Chem. Ber.* **1992**, *125*, 353−365.
(24) Chaplin, A. B.; Hooper, J. F.; Weller, A. S.; Willis, M. C. *J. Am. Chem. Soc.* **2012**, *134*, 4885−4897.
(25) Wass, D. F. *Dalton Trans.* **2007**, 816−819.
(26) Bowen, L. E.; Charernsuk, M.; Hey, T. W.; McMullin, C. L.; Orpen, A. G.; Wass, D. F. *Dalton Trans.* **2010**, *39*, 560−567.
(27) Theodor, A. *Coord. Chem. Rev.* **2011**, *255*, 861−880.
(28) Carter, A.; Cohen, S. A.; Cooley, N. A.; Murphy, A.; Scutt, J.; Wass, D. F. *Chem. Commun.* **2002**, 858−859.
(29) Maumela, M. C.; Blann, K.; de Bod, H.; Dixon, J. T.; Gabrielli, W. F.; Williams, D. B. G. *Synthesis* **2007**, 3863−3867.
(30) Wolf, J.; Manger, M.; Schmidt, U.; Fries, G.; Barth, D.; Weberndorfer, B.; Vicic, D. A.; Jones, W. D.; Werner, H. *J. Chem. Soc., Dalton Trans.* **1999**, 1867−1875.
(31) Fryzuk, M. D.; Jones, T.; Einstein, F. W. B. *Organometallics* **1984**, *3*, 185−191.
(32) Lubben, A. T.; McIndoe, J. S.; Weller, A. S. *Organometallics* **2008**, *27*, 3303−3306.
(33) Ellermann, J.; Hohenberger, E. F.; Kehr, W.; Purzer, A.; Thiele, G. *Z. Anorg. Allg. Chem.* **1980**, *464*, 45−66.
(34) Valderrama, M.; Contreras, R.; Boys, D. *J. Organomet. Chem.* **2003**, *665*, 7−12.
(35) Reves, M.; Ferrer, C.; Leon, T.; Doran, S.; Etayo, P.; Vidal-Ferran, A.; Riera, A.; Verdaguer, X. *Angew. Chem., Int. Ed.* **2010**, *49*, 9452−9455.
(36) Moxham, G. L.; Randell-Sly, H.; Brayshaw, S. K.; Weller, A. S.; Willis, M. C. *Chem.—Eur. J.* **2008**, *14*, 8383−8397.
(37) Chaplin, A. B.; Poblador-Bahamonde, A. I.; Sparkes, H. A.; Howard, J. A. K.; Macgregor, S. A.; Weller, A. S. *Chem. Commun.* **2009**, 244−246.
(38) Buchner, M. R.; Herdtweck, E.; Schneider, S. *J. Organomet. Chem.* **2008**, *693*, 3943−3946.
(39) Cooper, A. C.; Huffman, J. C.; Caulton, K. G. *Organometallics* **1997**, *16*, 1974−1978.
(40) Freixa, Z.; van Leeuwen, P. W. N. M. *Dalton Trans.* **2003**, 1890−1901.
(41) Wilson, A. D.; Miller, A. J. M.; DuBois, D. L.; Labinger, J. A.; Bercaw, J. E. *Inorg. Chem.* **2010**, *49*, 3918−3926.
(42) Zuidema, E.; Escorihuela, L.; Eichelsheim, T.; Carbó, J. J.; Bo, C.; Kamer, P. C. J.; van Leeuwen, P. W. N. M. *Chem.—Eur. J.* **2008**, *14*, 1843−1853.
(43) Beta-elimination in alkenyl intermediates is rare. See for example: Ghosh, R.; Zhang, X.; Achord, P.; Emge, T. J.; Krogh-Jespersen, K.; Goldman, A. S. *J. Am. Chem. Soc.* **2007**, *129*, 853.
(44) Ghosh, R.; Zhang, X.; Achord, P.; Emge, T. J.; Krogh-Jespersen, K.; Goldman, A. S. *J. Am. Chem. Soc.* **2007**, *129*, 853−866.
(45) A minor species, tentatively attributed to a $\kappa^1$-O-$\eta^2$-(C═C)-isomer is also observed, characterized by two up-field shifted alkene signals at $\delta$ 5.70 and $\delta$ 4.88 in the $^1$H NMR spectrum and a very similar set of resoances in the $^{31}$P{$^1$H} NMR spetcrum. These species are also observed on direct addition of the product to **6a** in acetone. See Supporting Information. We see no evidence for a C−S activated species, see for example: Hooper, J. F.; Chaplin, A. B.; González−Rodríguez; Thompson, A. L.; Weller, A. S.; Willis, M. C. *J. Am. Chem. Soc.* **2012**, *134*, 2906−2909.
(46) Schrock, R. R.; Osborn, J. A. *J. Am. Chem. Soc.* **1976**, *98*, 2143−2147.